Low CD4 nadir exacerbates the impacts of APOE ε4 on functional connectivity and memory in adults with HIV

Supplementary Material

Authors: Fan Nils Yang, PhD[1], Margarita Bronshteyn, B.A.[1], Sarah A. Flowers, PhD[1], Matthew Dawson, M.A.[4], Princy Kumar, MD[2], G. William Rebeck, PhD[1], R. Scott Turner, MD, PhD[3], David J. Moore, PhD[4], Ronald J. Ellis, MD, PhD[4,5], Xiong Jiang, PhD[1*]

Affiliations: [1]Departments of Neuroscience, [2]Department of Neurology, [3]Department of Medicine, Georgetown University Medical Center, Washington, DC 20057, USA; [4]Department of Psychiatry, [5]Department of Neurosciences, University of California, San Diego, La Jolla, CA 92093, USA.

Corresponding Author: Xiong Jiang, PhD, Department of Neuroscience, Georgetown University Medical Center, Washington, DC 20007, USA. (Xiong.Jiang@georgetown.edu).

SUPPLEMENTARY METHODS

Participants

One hundred and four persons with HIV (PWH) from the local communities participated in this study. Each participant was initially screened via telephone interview, which was followed by an onsite screening visit to ensure all the following criteria were met: aged from 41-70 years old; be able to speak and understand English; had more than seven years of education; had no MRI contraindications such as claustrophobia or metal implants; no illicit substance use within the past three months (urine toxicology tests were mandatory during each visit); and no other major neurological and psychiatric disorders (stroke, loss of consciousness for more than 30 minutes, or other HIV-unrelated neurological disorders). Three participants were excluded from data analysis due to the lack of genotype information (two declined to provide saliva samples, and a third had insufficient saliva volume). Two additional participants were excluded due to visible brain anomalies (McCune-Albright Syndrome (n=1) or suspected benign tumor (n=1)). Per IRB guideline, both participants were notified and the structural MRI images were sent to their primary physicians and/or radiologists. Similar but stronger results were obtained with inclusion of the two participants - both were APOE ε4 carriers with poor memory performance. In the end, a total of 99 participants were included in the final analysis, and all except two ε4 noncarriers were on stable cART during study visits. Self-reported CD4 nadirs were documented and used in data analysis. Previous studies have shown the self-reported CD4 nadir is largely accurate and strongly correlates with the actual medical records (if available) [1,2], even in a highly socially marginalized population [2]. Two of them were only able to provide the ranges of their CD4 nadirs, and in both cases, the medians of the ranges were used.

MRI acquisition and pre-processing

Structural MRI and resting-state functional MRI (fMRI) were acquired at the local institute using a 3-Tesla Siemens Magnetom Trio with a 12-channel head coil or Prisma-Fit scanner with a 20-channel head coil. The potential effects of different scanners were investigated and controlled (see the section of "**The effect of the scanner (Trio or Prisma-fit) on brain measurements"** for more details).

High-resolution T1-weighted images were acquired using a 3D-MPRAGE sequence with following parameters: $1\times1\times1mm^3$ resolution, TR/TE = 1900/2.52ms, flip angle = 9°, 160 contiguous 1mm sagittal slices, FoV = 256mm (256x256 matrix). One run of resting state fMRI images was acquired using an echo-planar sequence with following parameters: flip angle = 90°, TR/TE = 2040/29ms, FoV = 205mm (64×64 matrix), 35 interleaved axial slices (4mm thick, no gap; $3.2\times3.2mm^2$ in plane resolution). There were 264 acquisitions.

The software package SPM12 (https://www.fil.ion.ucl.ac.uk/spm/), the Computational Anatomy Toolbox (CAT, version 12.5) (www.neuro.uni-jena.de/cat/), and the CONN functional connectivity toolbox (https://www.nitrc.org/projects/conn/) [3] were used for pre-processing and analyzing structural and functional MRI data, respectively. Default processing pipeline settings of the CAT and CONN were applied.

Briefly, pipeline for processing structural MRI in CAT including bias-field inhomogeneities, denoising, skull-stripping, segmentation, and corrections for partial volume estimation. Cortical thickness was estimated using the projection-based thickness, and smoothed using 15mm full width at half maximum (FWHM) Gaussian filter. Modulated normalized gray matter volumes (GMv) were obtained to preserve voxel-wise estimates of the absolute amount of tissue, and then smoothed using an 8-mm FWHM Gaussian filter.

For resting-state fMRI, raw images were first preprocessed in SPM12. The preprocessing includes slice-timing correction, realignment, coregistration to structural volume, normalization based on structural normalization parameters obtained from CAT12, outlier identification, smoothing with an 8-mm FWHM (for standard ROI analyses) or without smooth (for subject-specific ROI analyses, see section below on ‘Construction of memory functional networks’). Then, normalized images were processed following the standard CONN pipeline [3]. The temporal processing in CONN includes movement regression, removal of signals from CSF and white matter, band passing [0.01 0.1] Hz, detrend, and a structural aCompCor strategy (during which, the distribution of correlation values will be approximately centered and normalized, see an example picture, Fig. S1).

Quality control (QC) of MRI images

All the MRI images, including T1 images in native space, normalized T1 images, resting-state BOLD images in native space, normalized resting-state BOLD images, were visually inspected by the authors. A binary quality rating for each image were created (0: fail, 1: pass). For T1 images, additional quality assurance rating generated by CAT12 was used: the overall rating must higher than 3.5 (i.e. higher than the satisfactory quality). For resting-state BOLD images, maximum movement in any direction or maximum rotation must be lower than 1mm or 1 degree, respectively (outlier acquisitions were scrubbed). Two subjects were excluded due to fail to pass QC, i.e., with visible brain anomalies (see Participants section).

Construction of regions of interest (ROIs)

The Papez circuit and bilateral caudate ROIs were used to define the memory-related network, adopting from an early ε4 study on cognitively intact middle-aged adults [4]. The Papez circuit includes the parahippocampal cortex (PHC), hippocampus (HIP), entorhinal cortex (EC), anterior thalamic nuclei, mammillary body (MB), and cingulate cortices [5]. Specifically, bilateral thalamus (THA), bilateral caudate (CAU), anterior cingulate cortex (ACC), and posterior cingulate cortex (PCC) ROIs were defined using the Automated Anatomical Labeling (AAL) template in the CONN toolbox. Bilateral mammillary body were defined using the CoBra template in the CAT toolbox. Given that HIP and other regions in the medial temporal lobe (MTL) have complex shape and moderate anatomical variability, subject-specific ROIs were obtained bilaterally for anterior HIP (aHIP), posterior HIP (pHIP), EC, and PHC, using the Automatic Segmentation of Hippocampal Subfields (ASHS) software package (https://www.nitrc.org/projects/ashs) [6]. See Fig. S2 for the right MTL sub-regions of one representative subject.

Construction of memory functional networks

Memory functional networks of each subject were constructed based on following criteria. First, time series of each ROI were extracted either using smoothed (for CAU, THA, ACC, and PCC

ROIs) or unsmoothed fMRI data (for mammillary body and subject-specific ROIs: aHIP, pHIP, EC, and PHC). As mammillary body is a relatively small region, unsmoothed fMRI data was used to reduce 'contamination' from neighboring voxels. Second, the FC between two time series of all pairwise ROIs was calculated using Pearson's Correlation and then the correlation coefficients were Fisher-transformed for further statistical analysis (all were done in the CONN toolbox).

Statistical analyses

The CAT software package was used to test the effect of ε4 status on cortical thickness and GMv, using a non-parametric permutation-based approach [7] at a threshold of $p<0.001$ (uncorrected, at least 50 contiguous voxels). See supplemental materials for detailed information.

Three types of FC analyses were conducted with the CONN software package: ROI-to-ROI, seed-to-voxel, and multivariate seed-to-voxel FC analyses.

The Papez circuit and bilateral caudate ROIs were identified, including THA, CAU, MB, aHIP, pHIP, EC, PHC, ACC, and PCC. The ROI-to-ROI FC analyses of the left and right hemisphere were conducted separately, with ACC and PCC were included in the analyses of both hemispheres. A threshold of $p<0.05$ (false discovery rate (FDR) corrected) was applied in ROI-to-ROI FC analysis.

Next, we investigated the correlations between ROI-to-ROI FCs with significant group differences and the two neuropsychological test scores (HVLT-R retention and delayed recall scores). Additional permutation test was conducted to test whether the correlation coefficient was higher/lower than zero with 10000 permutations by randomly shuffling one of the two variables [8]. Then, a General Linear Model (GLM) was performed to examine the potential interaction between ε4 status and HIV disease on FC, with the FC between CAUr and aHIPr (the only ROI-to-ROI FC with a significant group difference as well as a significant correlation with HVLT-R retention rate) as the dependent variable; and HIV disease measurements (current CD4, or CD4 nadir, or disease duration, separately), ε4 status, ε4 status × HIV disease, age, education, sex, and race as the independent variables.

Additional seed-to-voxel FC and multivariate seed-to-voxel analyses were performed to further investigate the impacts of ε4 status on brain functional network. Based on the results of ROI-to-ROI FCs, the right caudate (CAUr) and the right anterior hippocampus (aHIPr) were chosen as the seed ROIs, respectively. Seed-to-voxel FC analyses were thresholded at voxel-wise $p<0.001$ uncorrected, cluster-wise $p<0.05$ FDR corrected.

To further compare the roles of the right caudate (CAUr) and the right anterior hippocampus (aHIPr) in the functional network disruptions, multivariate seed-to-voxel analyses were conducted. When the right caudate (CAUr) was chosen as the seed region, the BOLD timeseries of the right anterior hippocampus (aHIPr) were included as covariate to control for contribution from aHIPr. Similarly when the right anterior hippocampus (aHIPr) was chosen as the seed region, the BOLD timeseries of the right caudate (CAUr) were included as covariate. The multivariate seed-to-voxel FC analyses were thresholded at voxel-wise $p<0.001$ uncorrected, cluster-wise $p<0.05$ FDR corrected.

The effect of the scanner (Trio or Prisma-fit) on brain measurements

During the study period, the scanner was upgraded from Siemens 3-Tesla Trio to Prisma-Fit (n=57 with the original MRI system, and n=42 with the new MRI system). The potential effect of the scanner on gray matter volume (GMv), cortical thickness, and functional connectivity (FC) was examined with two independent approaches.

In the first approach, scanner was coded as binary covariance (0=Trio, 1=Prisma-Fit) for MRI data analyses; adding the scanner as an additional covariate did no change the results of GMv, cortical thickness, and FC. In addition, the interaction effect of APOE genotype and the scanner on the FC (between CAUr and aHIPr) was not significant ($F(1,91)=0.15$, $p=0.7$), after controlling for age, education, sex, and race.

In the second approach, modified ComBat [9,10], an advanced technique that is specifically designed to control for the potential effect of scanners in multi-site studies, was applied to minimalize potential biases and non-biological variability on FC induced by the scanner. In this analysis, connectivity matrix of two 9x9 ROIs was built. The upper triangle of this matrix was created for each subject and was used in ComBat, with age, education, sex, and race as covariates. The difference on the CAUr-aHIPr FC ($FC_{CAUr\text{-}aHIPr}$) between APOE ε4 carriers and noncarriers was comparable before ($F(1,93) = 12.42$, $p = 0.0007$) or after applying ComBat ($F(1,93) = 12.51$, $p = 0.0006$).

Therefore, we concluded that the effect of scanner on MRI data was minimal in the study and did not interfere with the study results and conclusions.

SUPPLEMENTARY RESULTS

Moderated mediation analysis

In the moderated mediation analysis, we examined whether the ε4 effect on the memory network FC ($FC_{CAUr\text{-}aHIPr}$) had implications (indirect effect) for memory performance (HVLT-R retention), and whether the indirect effect was conditional on CD4 nadir (Fig. 5a). The analysis revealed a significant moderated mediation effect (index = 0.009) with 95% confidence interval (CI) ranging from 0.0002 to 0.0221, which did not encompass zero, suggesting a significant model (Fig. 5b).

Specifically, c′, the direct effect of X (ε4 status) on Y (HVLT-R retention) was approaching significance ($t(92)=-1.96$, $p=0.052$); b, the effect of mediator M ($FC_{CAUr\text{-}aHIPr}$) on Y was significant ($t(92)=-2.06$, $p=0.042$). In addition, a_1, the effect of X on M was significant ($t(90)=-3.99$, $p=0.00013$); a_2, the effect of W (CD4 nadir) on M was not significant ($t(90)=-0.53$, $p=0.598$); and a_3, the interaction effect between X and W on M was significant ($t(90)=2.96$, $p=0.004$), suggesting that carriers had lower $FC_{CAUr\text{-}aHIPr}$ than noncarrriers, but only if their CD4 nadirs were low, in line with the results in Fig. 4a. Furthermore, the indirect effect of X on Y was contingent on the values of moderator W (CD4 nadir): if W = 30.04 (16^{th} percentile), the indirect effect (C1=-4.00) was significantly below zero (95% CI: [-9.42 -0.09]); if W =199.5 (median value), the indirect effect (C2=-2.50) was significantly below zero (95% CI: [-5.95 -0.06]); if W =462.4 (84^{th} percentile), the indirect effect (C3=-0.16) was not significant (95% CI: [-2.17 1.39]). That is, the indirect effect of X (ε4 status) on Y (HVLT-R retention) through M ($FC_{CAUr\text{-}aHIPr}$) was significant only when W (CD4 nadir) was low (i.e., 199.5 cells/μl or lower).

SUPPLEMENTARY REFERENCES

1 Ellis RJ, Badiee J, Vaida F, Letendre S, Heaton RK, Clifford D, *et al.* **CD4 nadir is a predictor of HIV neurocognitive impairment in the era of combination antiretroviral therapy**. *AIDS* 2011; **25**:1747–1751.

2 Buisker TR, Dufour M-SK, Myers JJ. **Recall of Nadir CD4 Cell Count and Most Recent HIV Viral Load Among HIV-Infected, Socially Marginalized Adults**. *AIDS Behav* 2015; **19**:2108–2116.

3 Whitfield-Gabrieli S, Nieto-Castanon A. **Conn: a functional connectivity toolbox for correlated and anticorrelated brain networks.** *Brain connectivity* 2012; **2**:125–41.

4 Li W, Antuono PG, Xie C, Chen G, Jones JL, Ward BD, *et al.* **Aberrant functional connectivity in Papez circuit correlates with memory performance in cognitively intact middle-aged APOE4 carriers**. *Cortex* 2014; **57**:167–176.

5 Jicha GA, Carr SA. **Conceptual evolution in Alzheimer's disease: Implications for understanding the clinical phenotype of progressive neurodegenerative disease**. *J Alzheimers Dis* 2010; **19**:253–272.

6 Yushkevich PA, Pluta JB, Wang H, Xie L, Ding S-L, Gertje EC, *et al.* **Automated volumetry and regional thickness analysis of hippocampal subfields and medial temporal cortical structures in mild cognitive impairment**. *Hum Brain Mapp* 2015; **36**:258–287.

7 Smith SM, Nichols TE. **Threshold-free cluster enhancement: Addressing problems of smoothing, threshold dependence and localisation in cluster inference**. *NeuroImage* 2009; **44**:83–98.

8 Manly BFJ. *Randomization, Bootstrap and Monte Carlo Methods in Biology*. Chapman and Hall/CRC; 2018. doi:10.1201/9781315273075

9 Johnson WE, Li C, Rabinovic A. **Adjusting batch effects in microarray expression data using empirical Bayes methods**. *Biostatistics* 2007; **8**:118–127.

10 Yu M, Linn KA, Cook PA, Phillips ML, McInnis M, Fava M, *et al.* **Statistical harmonization corrects site effects in functional connectivity measurements from multi-site fMRI data**. *Human Brain Mapping* 2018; **39**:4213–4227.

11 Nyberg L, Karalija N, Salami A, Andersson M, Wåhlin A, Kaboovand N, *et al.* **Dopamine D2 receptor availability is linked to hippocampal-caudate functional connectivity and episodic memory**. *Proc Natl Acad Sci USA* 2016; **113**:7918–7923.

12 Whitfield-Gabrieli SL, Nieto-Castañón A. **Conn: A Functional Connectivity Toolbox for Correlated and Anticorrelated Brain Networks**. *Brain connectivity* 2012; **2**:125–141.

SUPPLEMENTARY TABLES

Table S1. Individual neuropsychological test scores (mean (SD)) and GMv of MTL subregions in APOE ε4 carriers and noncarriers. Groups difference was examined using ANOCOVA, after controlling age, education (number of years), sex, and race. BVMT-R, Brief Visuospatial Memory Test-Revised; COWAT, Controlled Oral Word Association Test; HVLT-R, Hopkins Verbal Learning Test-Revised; MOCA, Montreal Cognitive Assessment; NP, neuropsychological; WAISIII, Wechsler Adult Intelligence Scale III; WCST, Wisconsin Card Sorting Test; WRAT4, Wide Range Achievement Test 4 reading; EC, entorhinal cortex; PHC, parahippocampal cortex.

Cognitive domains	NP tests	Carriers	Noncarriers	p-value*
General Cognition	MoCA _	22.77 (3.5)	24.33 (4.0)	n.s.
Verbal fluency and Reading skills	Animal Fluency	20.31 (4.1)	20.51 (4.5)	n.s.
	COWAT: F	13.58 (5.3)	14.03 (4.3)	n.s.
	COWAT: A	10.81 (4.0)	11.08 (4.0)	n.s.
	COWAT: S	14.50 (4.8)	14.48 (5.2)	n.s.
	WRAT4	54.69 (9.8)	58.49 (10.3)	n.s.
Executive function	STROOP: Color	59.65 (11.5)	63.10 (12.4)	n.s.
	STROOP: Word	83.08 (19.2)	85.74 (16.1)	n.s.
	STROOP: Color&Word	31.23 (9.4)	33.70 (10.3)	n.s.
	Trail Making B (secs)	102.42 (61.2)	107.90 (71.6)	n.s.
	WCST	36.12 (10.7)	35.19 (12.5)	n.s.
Speed of information processing	WAISIII DigiSymbol_	60.2 (12.5)	61.8 (14.7)	n.s.
	Trail Making A(secs)	28.7 (9.9)	31.8 (13.0)	n.s.
Attention/Working memory	WAISIII Symbol Search_	26.4 (5.5)	27.7 (8.3)	n.s.
	WAISIII Line Number Sequencing_	7.77 (3.7)	8.49 (2.9)	n.s.
Learning	HVLT-R: Total Recall_	22.58 (4.7)	25.44 (5.0)	n.s.
	HVLT-R: Discrimination Index	9.12 (2.0)	10.12 (2.1)	n.s.
	BVMT-R:Total Recall	16.35 (7.2)	17.03 (6.9)	n.s.
	BVMT-R: Discrimination Index_	5.15 (1.2)	5.49 (1.0)	n.s.
Memory	HVLT-R: Delayed Rrecall	6.96 (2.6)	8.63 (2.5)	0.009#
	HVLT-R: Retention Rate (%)	74.3 (18.6)	85.8 (15.3)	0.002#
	BVMT-R: Delayed Recall	6.35 (2.9)	7.15 (2.8)	n.s.
	BVMT-R: Retention Rate (%)	84.1 (22.9)	95.9 (15.6)	n.s.
Motor skills	GroovedPegBoard: Dominant (sec) _	82.0 (19.1)	84.6 (32.7)	n.s.
	GroovedPegBoard: NonDominant (sec)	97.0 (27.9)	95.0 (37.1)	n.s.
MTL subregions	left_Anterior_hippocampus	1592.2 (293.6)	1577.0 (263.6)	n.s.
	left_Posterior_hippocampus	1713.1 (216.6)	1694.2 (210.3)	n.s.

	left_EC	589.7 (114.1)	578.1 (100.4)	n.s.
	Left PHC	1014.7 (157.6)	1012.9 (174.4)	n.s.
	right_Anterior_hippocampus	1702.6 (329.5)	1710.5 (285.0)	n.s.
	right_Posterior_hippocampus	1669.5 (226.6)	1653.0 (206.1)	n.s.
	right_EC	592.7 (124.2)	583.5 (89.7)	n.s.
	right_PHC	1033.4 (157.3)	1015.2 (159.6)	n.s.

[*] n.s., non-significant. [#] Two outliers identified using the MATLAB *isoutlier* function in Fig. 1 were excluded.

Table S2. Demographics and HIV disease information of the subgroup of PWH who had undetectable viral load. To examine whether the impact of APOE ε4 on brain function and network persists in PWH with undetectable viral load, we identified and conducted similar analyses on the subset of PWH with undetectable viral load (<20 copies/mL in blood specimens) (n=82). All of the participants in the subgroup were also on stable cART. Similar results were observed in the clinically relevant subgroup (see Fig. S3 to S6).

	Carriers (n=22)	**Noncarriers (n=60)**	***p*-value**
Age (yrs)	55.1 (6.3) [a]	56.8 (6.9)	n.s. [b]
Education (yrs)	13.6 (3.0)	14.8 (3.0)	n.s.
Sex (Female%)	22.7%	23.3%	n.s.
Race (AA%) [c]	77.3%	55.0%	n.s.
Current CD4 (cells/µl)	694.5 (550)	712 (501)	n.s.
CD4 nadir (cells/µl)	152 (330)	200 (262.5) [d]	n.s.
Disease duration (yrs)	25.5 (10.1)	25.6 (9.2)	n.s.
GDS [e]	0.32 (0.27)	0.34 (0.47)	n.s.
HAND diagnosis [f]	27.3%	25.0%	n.s.

Note: [a] Age, education, disease duration, and GDS were presented as mean (standard deviation), versus current CD4 and CD4 nadir were presented as median (IQR); [b] n.s., not significant; [c] AA, African-Americans; [d] median (IQR), and one noncarrier did not provide CD4 nadir (treated as a missing value); [e] GDS, global deficits score, which was calculated from the seven neurocognitive domains; [f] HAND, HIV-associated neurocognitive disorders.

Table S3. Demographics and HIV disease information of the African-American (AA) subgroup of PWH. To examine the impact of APOE ε4 on brain function and network in African Americans with HIV, we identified and conducted similar analyses on the AA subgroup (n=62). Similar results were observed in the AA subgroup (see Fig. S7 to S10).

	Carriers (n=20)	**Noncarriers (n=42)**	***p*-value**
Age (yrs)	54.7 (6.3) [a]	57.8 (6.5)	n.s. [b]
Education (yrs)	12.7 (2.8)	13.1 (2.6)	n.s.
Sex (Female%)	35.0%	31.0%	n.s.
Race (AA%) [c]	100%	100%	n.s.
Current CD4 (cells/µl)	694.5 (563)	581 (363)	n.s.
CD4 nadir (cells/µl)	109.5 (256.5)	190 (261.8) [d]	n.s.
Disease duration (yrs)	29.4 (6.2)	28.3 (8.7)	n.s.
GDS [e]	0.27 (0.27)	0.22 (0.29)	n.s.
HAND diagnosis [f]	15.0%	9.5%	n.s.

Note: [a] Age, education, disease duration, and GDS were presented as mean (standard deviation), versus current CD4 and CD4 nadir were presented as median (IQR); [b] n.s., not significant; [c] AA, African-Americans; [d] median (IQR), and one noncarrier did not provide CD4 nadir (treated as a missing value); [e] GDS, global deficits score, which was calculated from the seven neurocognitive domains; [f] HAND, HIV-associated neurocognitive disorders.

SUPPLEMENTARY FIGURES

Figure S1. Effect of temporal preprocessing steps on the distribution of voxel-to-voxel BOLD signal correlation values of a representative subject. Upper panel, the distribution of correlation values was skewed towards right hand side (mean value 0.20). Bottom panel, the distribution of correlation values was approximately centered and normalized (mean value 0.05). The shift in distribution and mean was expected with algorithms implemented in the CONN toolbox [12].

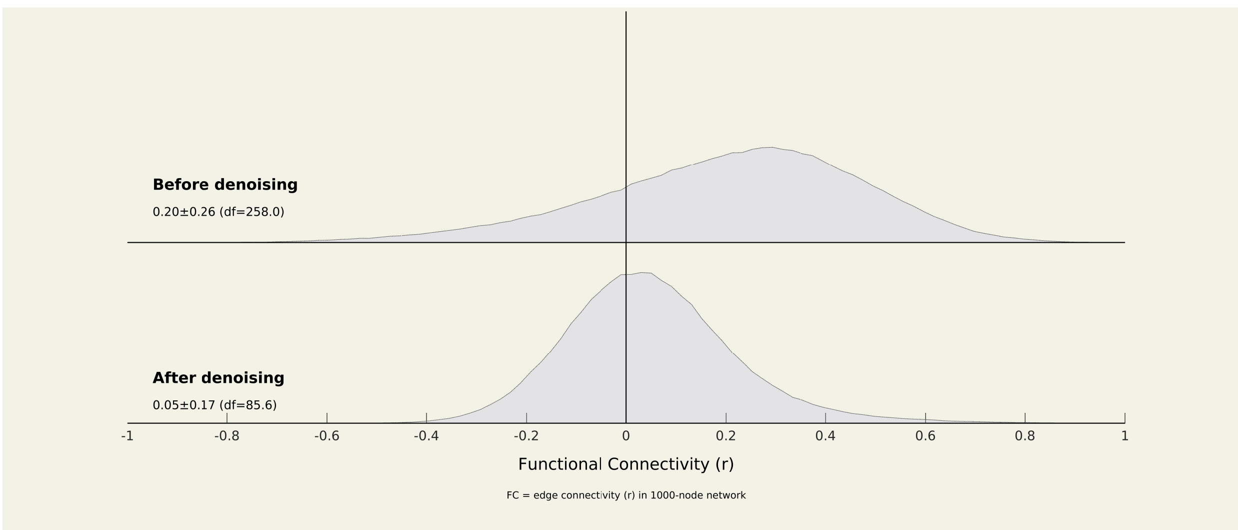

Figure S2. Segmentation of the right MTL sub-regions in one representative subject. The Automatic Segmentation of Hippocampal Subfields (ASHS) software package [6] was used for the segmentation of MTL subregions**.** Red: anterior hippocampus; lime green: posterior hippocampus; purple: parahippocampal cortex; light green: entorhinal cortex; light blue: BA35; dark blue: BA 36; gray: collateral sulcus; brown: occipitemporal sulcus; pink: dura; orange: meninges.

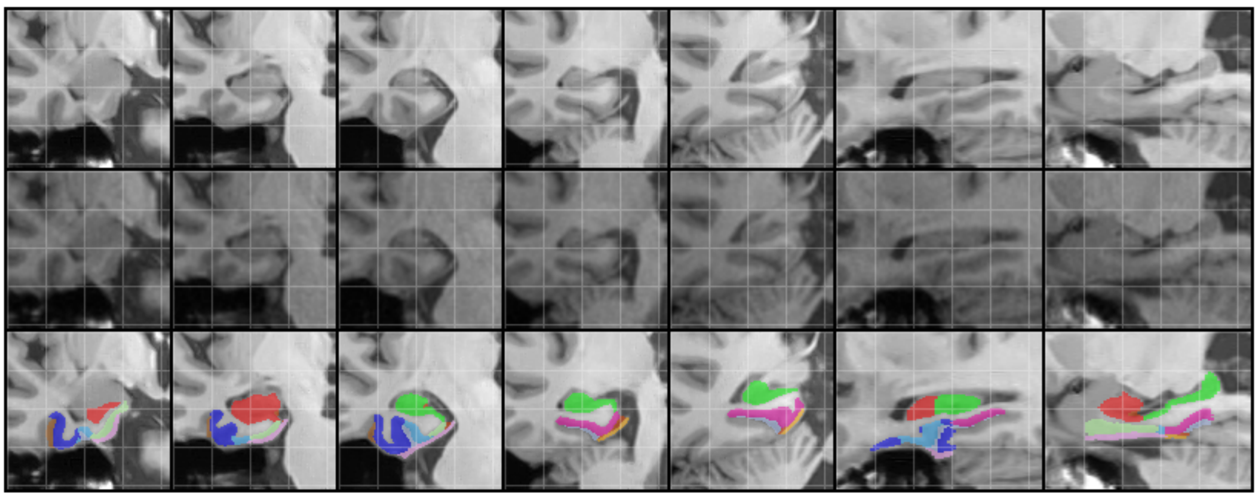

Figure S3. Group differences in HVLT-R retention and delayed recall in the subset of subjects (n=82) with undetectable viral load in their blood specimens. (A) APOE ε4 carriers (red circles) has significantly lower HVLT-R retention as compared to noncarriers (blue circles; blue crosses denote outliers that outside 3 median absolute deviations of the median value), *p*=0.005; (B) a marginal difference the difference APOE ε4 carriers (red circles) has significantly lower HVLT-R delayed recall as compared to noncarriers (blue circles), *p*=0.040. On each box, the central mark (red line) referred to the median, and the bottom and top edges of the box indicate the 25th and 75th percentiles, respectively. The whiskers extend to the most extreme data points not considered outliers. The results were similar to the entire study sample (Fig. 1). * denotes that two outliers found in retention (blue crosses) were excluded.

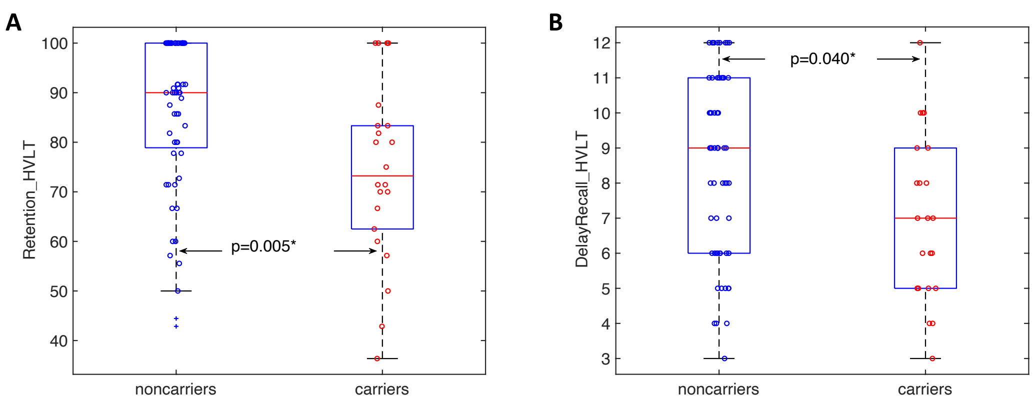

Figure S4. ROI-to-ROI functional connectivity (FC) analysis revealed reduced FC in ε4 carriers than noncarriers (undetectable viral load in both groups). The group comparisons (carriers versus noncarriers) of the ROI-to-ROI FC in the (A) left and (B) right hemisphere, respectively (each with nine ROIs). Both bilateral ACC and bilateral PCC were treated as single ROIs and were included in FC analyses in each hemisphere. The pairwise ROI-to-ROI FC comparisons that reached significant difference (with FDR correction) were highlighted with a red square box □. The colormap represented negative log *p*-values of group comparisons. APOE ε4 carriers had significant lower FCs between CAUr and aHIPr, pHIPr, THAr, and PHCr than carriers. Abbreviations: ACC/PCC, anterior/posterior cingulate cortex; aHIP/pHIP, anterior/posterior hippocampus; CAU, caudate; FC, functional connectivity; FDR, false discovery rate; MB, mammillary body; OC, occipital cortex; ROI, region-of-interest; PUT, putamen. THA, thalamus; -l/-r: left/right (e.g., CAUl/CAUr, left and right caudate, respectively).

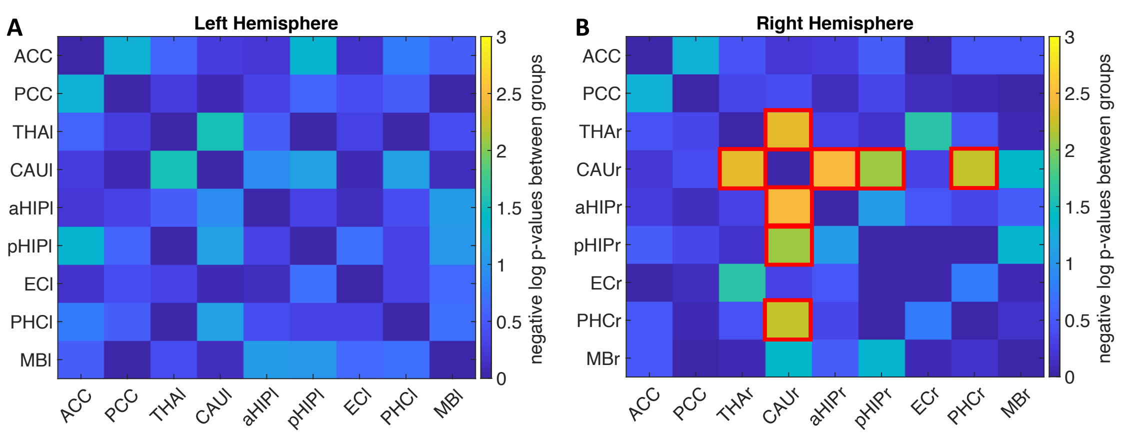

Figure S5. The correlation between HVLT-R retention scores and adjusted CAUr-to-aHIPr FC in the subgroup of PWH with undetectable viral load. Pearson correlation revealed a significant correlation (r=0.243, p=0.028, $p_{permutation}$=0.024 with 10000 permutations) between the adjusted $FC_{CAUr-aHIPr}$ and adjusted HVLT-R retention (adjusted for age, education, sex, and race). Red circles, carriers; blue circles, noncarriers.

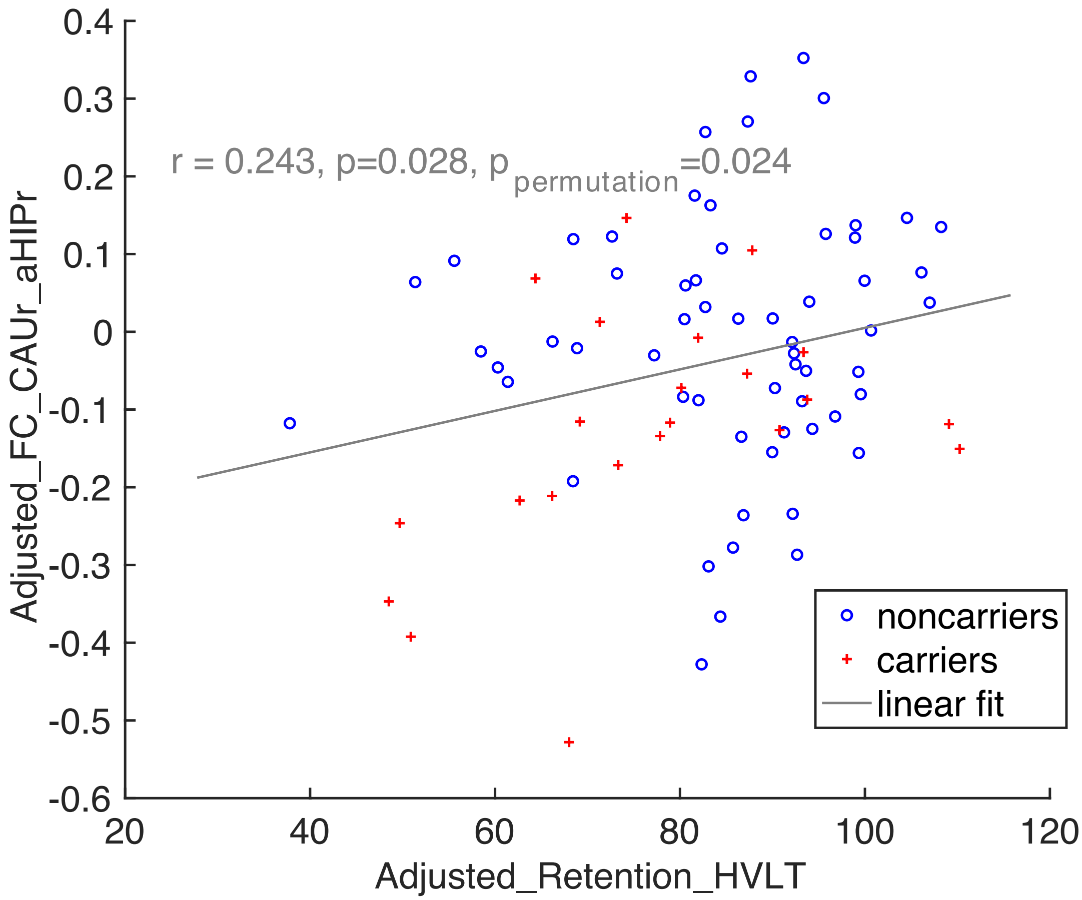

Figure S6. The interaction between APOE ε4 status and CD4 nadir on FC between CAUr and aHIPr in the subgroup of PWH with undetectable viral load. GLM revealed a significant interaction of APOE ε4 status and CD4 nadir on FC between CAUr and aHIPr ($F(1,73)=5.36$, $p=0.023$, the cyan text in the figure), after controlling for age, education, sex, and race. Post-hoc analyses revealed a significant correlation between FC and CD4 nadir in ε4 carriers ($r=0.523$, $p=0.013$, $p_{permutation}=0.011$ with 10000 permutations), but not in noncarriers ($p=0.603$, $p_{permutation}=0.585$ with 10000 permutations). For carriers: red circles, data of each individual subject; red line, fitted regression line; red text, correlation coefficient between FC and CD4 nadir in carriers. Noncarriers were shown in blue color.

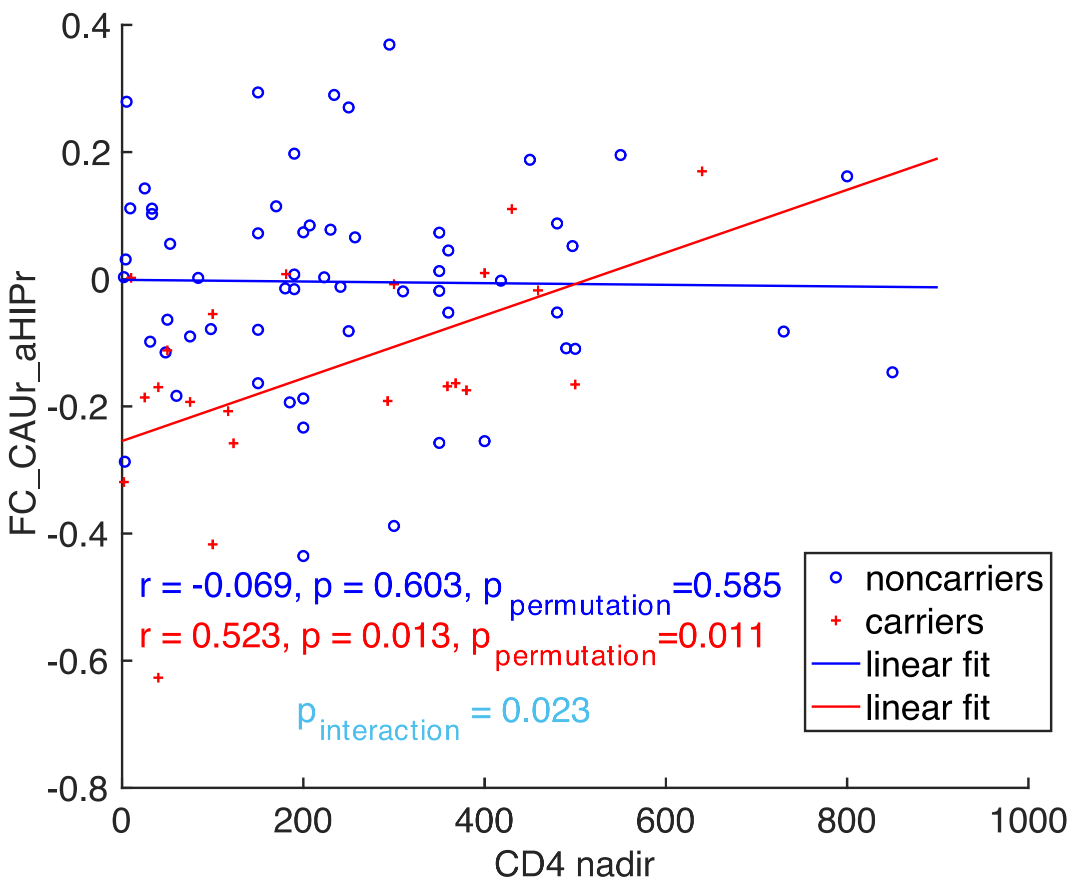

Figure S7. Group differences in HVLT-R retention and delayed recall in African-American (AA) subjects (n=62). (A) APOE ε4 carriers (red circles) has significantly lower HVLT-R retention as compared to noncarriers (blue circles), *p*=0.023; (B) a marginal difference the difference APOE ε4 carriers (red circles) has significantly lower HVLT-R delayed recall as compared to noncarriers (blue circles), *p*=0.059. On each box, the central mark (red line) referred to the median, and the bottom and top edges of the box indicate the 25th and 75th percentiles, respectively. The whiskers extend to the most extreme data points not considered outliers. The results were similar to the entire study sample (Fig. 1).

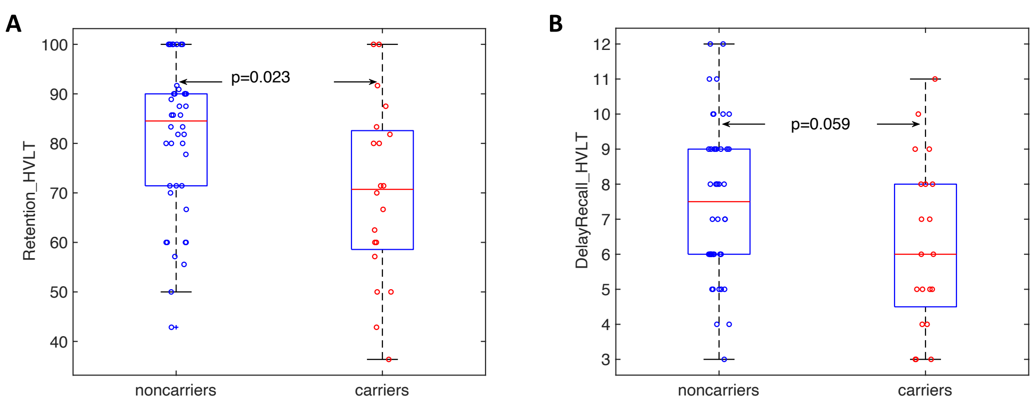

Figure S8. ROI-to-ROI functional connectivity (FC) analysis revealed reduced FC in ε4 carriers than noncarriers in the AA subgroup. The group comparisons (carriers versus noncarriers) of the ROI-to-ROI FC in the (A) left and (B) right hemisphere, respectively (each with nine ROIs). Both bilateral ACC and bilateral PCC were treated as single ROIs and were included in FC analyses in each hemisphere. The pairwise ROI-to-ROI FC comparisons that reached significant difference (with FDR correction) were highlighted with a red square box □. The colormap represented negative log *p*-values of group comparisons. APOE ε4 carriers had significant lower FCs between CAUr and aHIPr, pHIPr than carriers. Abbreviations: ACC/PCC, anterior/posterior cingulate cortex; aHIP/pHIP, anterior/posterior hippocampus; CAU, caudate; FC, functional connectivity; FDR, false discovery rate; MB, mammillary body; OC, occipital cortex; ROI, region-of-interest; PUT, putamen. THA, thalamus; -l/-r: left/right (e.g., CAUl/CAUr, left and right caudate, respectively).

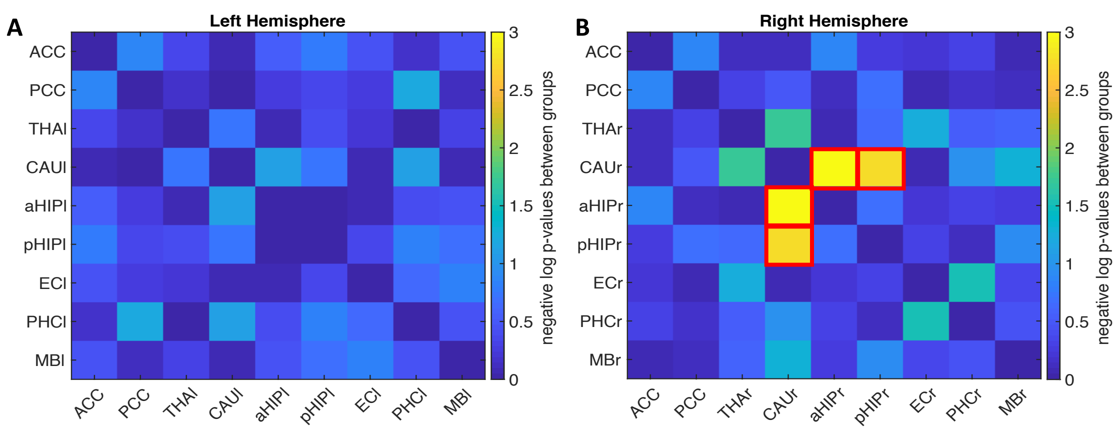

Figure S9. The correlation between HVLT-R retention scores and adjusted CAUr-to-aHIPr FC in the AA subgroup. Pearson correlation revealed a significant correlation (*r*=0.250, *p*<0.050, $p_{permutation}$=0.048 with 10000 permutations) between the adjusted $FC_{CAUr\text{-}aHIPr}$ and adjusted HVLT-R retention (adjusted for age, education, and sex). Red circles, carriers; blue circles, noncarriers.

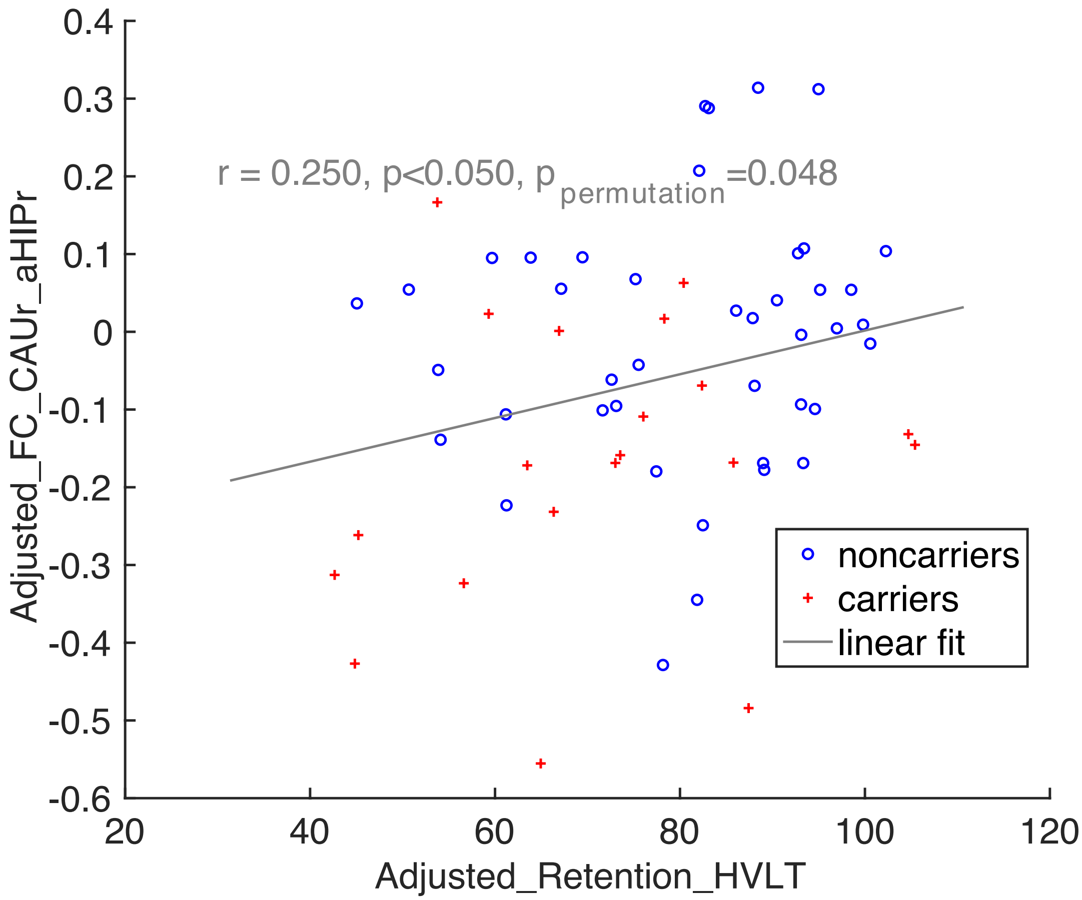

Figure S10. The interactive effect of APOE ε4 status and CD4 nadir on FC between CAUr and aHIPr in the AA subgroup. GLM revealed a significant interaction of APOE ε4 status and CD4 nadir on FC between CAUr and aHIPr ($F(1,54)=5.28$, $p=0.137$, the cyan text in the figure), after controlling for age, education, and sex. Post-hoc analyses revealed a significant correlation between FC and CD4 nadir in ε4 carriers (r=0.339, $p=0.144$, $p_{permutation}=0.138$ with 10000 permutations), but not in noncarriers (p=0.895, $p_{permutation}$ =0.876 with 10000 permutations). For carriers: red circles, data of each individual subject; red line, fitted regression line; red text, correlation coefficient between FC and CD4 nadir in carriers. Noncarriers were shown in blue color.

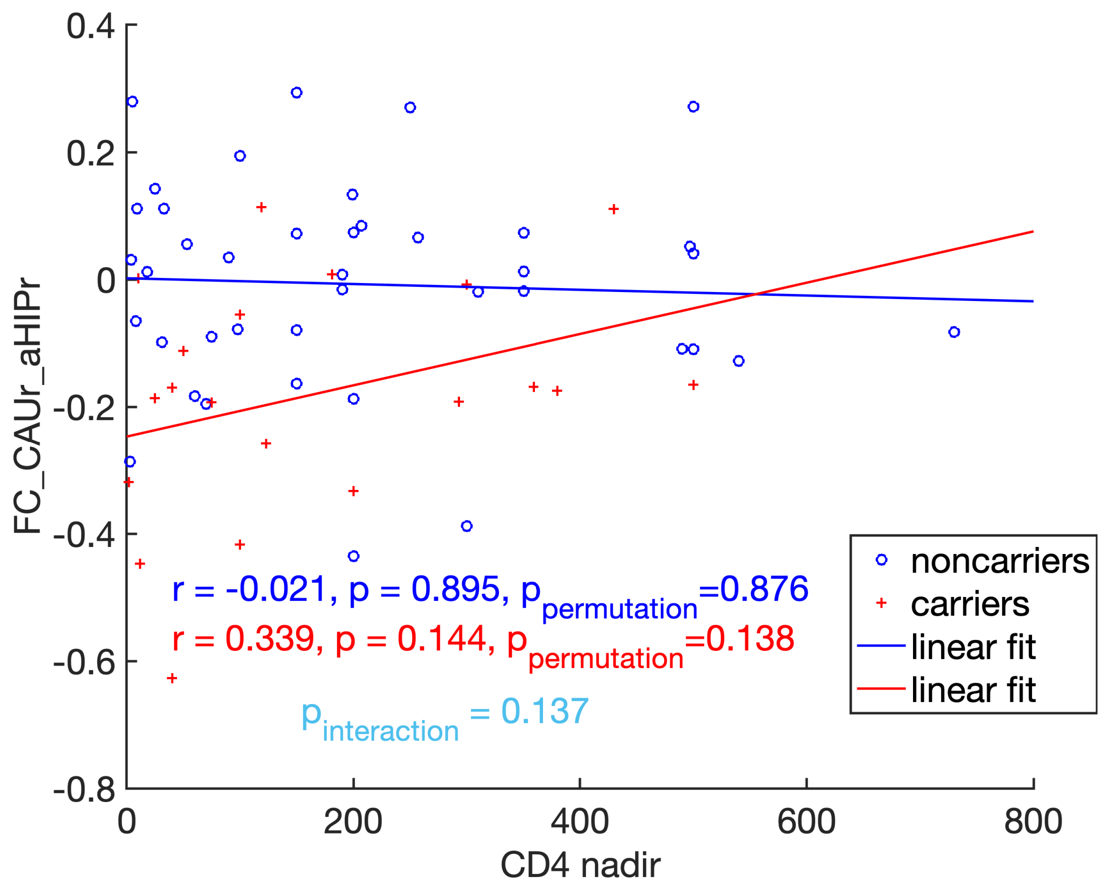

Figure S11. Background and hypothesis. (**A**) Background [4,11] – the relationship between APOE ε4, functional connectivity (FC), and episodic memory in HIV-uninfected adults. The moderated mediation analysis in the present study was motivated by many previous findings, especially two resting state fMRI studies that investigated the relationship between resting state functional connectivity (FC) and memory performance. In one study [4], Li et al. (2014) found that the FCs between hippocampus and caudate, and between hippocampus and other key regions of the Papez circuit were lower in cognitively normal middle-aged APOE ε4 carriers than noncarriers, even though there was no significant difference in memory performance between the two groups. Furthermore, across all subjects, FC between the hippocampus and caudate ($FC_{HIP-CAU}$) correlated with memory performance, suggesting a direct link between memory performance and $FC_{HIP-CAU}$. In another study [11], Nyberg et al. (2016) used a mediation analysis to investigate the relationship between D2 dopamine receptors at the caudate ($D2DR_{Cau}$), $FC_{HIP-CAU}$, and episodic memory in healthy older adults (64 to 68 y.o.). They found that $D2DR_{Cau}$ correlated with memory performance, and the relationship between $D2DR_{Cau}$ and memory performance was mediated through $FC_{HIP-CAU}$. Taken the two studies together, we proposed a potential model depicting the probable relationship between APOE ε4, $FC_{HIP-CAU}$, and episodic memory in HIV-uninfected adults. (**B**) Hypothesis – the relationship between APOE ε4, functional connectivity (FC), and episodic memory in adults with HIV. In PWH, it is known that low CD4 nadir is a strong predicator of neurocognitive impairment [23–26], therefore, we hypothesized that the relationship between APOE ε4 and $FC_{HIP-CAU}$ could be moderated by the CD4 nadir counts (or HIV-disease in general). More specifically, based on the results in Fig. 2 and 3 in the main article, we focused on the FC between the right anterior hippocampus and the right caudate ($FC_{CAUr-aHIPr}$) and tested whether low CD4 nadir exacerbates the effect of ε4 on the memory network ($FC_{CAUr-aHIPr}$) and memory performance. CAU, caudate; CAUr, right caudate; HIP, hippocampus; aHIPr, the right anterior hippocampus; FC, functional connectivity.